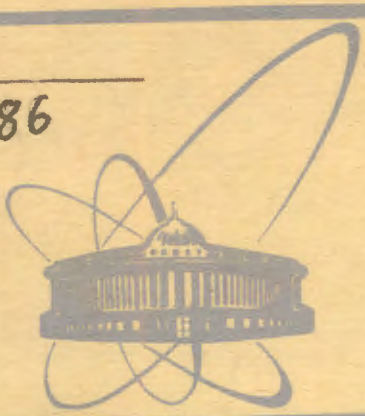

объединенный
институт
ядерных
исследований
дубна

E7 - 12411

V.V.Volkov, A.G.Artukh, L.P.Chelnokov,
G.F.Gridnev, A.N.Mezentsev, V.L.Mikheev,
A.Popescu, D.G.Popescu, A.M.Sukhov

SOME REGULARITIES OF THE DISINTEGRATION OF THE DOUBLE NUCLEAR SYSTEM IN THE REACTION 282 MeV ^{40}Ar + Ag

1979

E7 - 12411

V.V.Volkov, A.G.Artukh, L.P.Chelnokov,
G.F.Gridnev, A.N.Mezentsev, V.L.Mikheev,
A.Popescu,* D.G.Popescu,* A.M.Sukhov

SOME REGULARITIES OF THE DISINTEGRATION OF THE DOUBLE NUCLEAR SYSTEM IN THE REACTION 282 MeV ^{40}Ar + Ag

Submitted to "Nuclear Physics"

* On leave from the CIP, Bucharest

Волков В.В. и др.

E7 - 12411

Некоторые закономерности распада двойной ядерной системы в реакции 285 МэВ $^{40}Ar + Ag$

Изучались глубоконеупругие передачи в системе $^{107,109}Ag + ^{40}Ar$/285 МэВ/. Измерены энергетические спектры и сечения образования 87 изотопов с $2 \leq Z \leq 17$ для углов вылета 40^{o}. Показано, что для изотопов легких элементов (He - O) Q_{gg} -систематика выполняется удовлетворительно. Для более тяжелых элементов Q_{gg} -систематика нарушается из-за влияния вторичных ядерных процессов. Сделаны оценки энергии теплового возбуждения легких фрагментов по отклонению сечений образования легких фрагментов от Q_{gg}-систематики. Установлено сильное влияние ядерной структуры легкого фрагмента на величину сечения его образования. Выявлено сильное доминирование канала реакций передачи с вылетом α-частицы над остальными каналами многонуклонных передач. Сделаны оценки динамической деформации тяжелых фрагментов в глубоконеупругих передачах.

Работа выполнена в Лаборатории ядерных реакций, ОИЯИ.

Препринт Объединенного института ядерных исследований. Дубна 1979

Volkov V.V. et al.

E7 - 12411

Some Regularities of the Disintegration of the Double Nuclear System in the Reaction 285 MeV $^{40}Ar + Ag$

Deep inelastic transfer reactions have been studied in the system $^{107,109}Ag + ^{40}Ar$ at 285 MeV. The energy spectra and production cross sections for 87 isotopes of $2 \leq Z \leq 17$ have been measured at an emission angle of 40^{o}. It is shown that the Q_{gg}-systematics are satisfied for the isotopes of light elements from He to O. For the heavier elements the Q_{gg}-systematics are violated because of sequential nuclear processes. The excitation energy of light fragment is estimated from the deviation of production cross sections for light fragments from the Q_{gg}-systematics. It has been found that the nuclear structure of the light fragment strongly influences its production cross section. It has been established that the reaction channel involving α-particle emission strongly dominates over all the rest multinucleon transfer reaction channels. The dynamical deformation of heavy fragments in deep inelastic transfer reactions has been estimated.

The investigation has been performed at the Laboratory of Nuclear Reactions, JINR.

Preprint of the Joint Institute for Nuclear Research. Dubna 1979

1. INTRODUCTION

Studies of the interactions between heavy ions and nuclei have led to the discovery of a new type of nuclear reaction - deep inelastic transfers (DIT)*. The dynamical and statistical regularities characteristic of direct reactions and the decay of an excited compound nucleus are interwoven in the DIT mechanism. The twofold nature of DIT reactions is conditioned by the formation of a specific nuclear complex - a double nuclear system (DNS). The nuclei incorporated in the DNS interact intensively with each other by exchanging energy and nucleons, but they retain their identity to some extent. In DIT reactions, the Coulomb and centrifugal forces exceed the attractive forces acting between the nuclei, and this leads to the disintegration of the DNS. However, its disintegration proceeds rather slowly for 10^{-21} - 10^{-20} sec, owing to high nuclear viscosity. This period of time is long enough for the system to establish partial statistical equilibrium with respect to such degrees of freedom as thermal excitation energy and the neutron to proton ratio. However, the DNS does not reach full statistical equilibrium. A characteristic feature of the DNS is its evolution, which manifests itself in the redistribution of nucleons, angular momentum and excitation energy between the nuclei, as well as in the dynamical deformation of the system.

In the present paper, on the basis of the experimental data obtained for the system $^{107,109}Ag + ^{40}Ar$ (285 MeV) we consider some regularities of the evolution and disintegration of the DNS, i.e.,

(i) the validity of the Q_{gg}-systematics for DIT reactions induced by argon ions;

*Experimental and theoretical data on DIT reactions are reviewed in refs. /1-7/.

(ii) the distribution of thermal excitation energy between the DNS fragments;

(iii) the effect of the nuclear structure of light fragments on the characteristics of DIT reactions;

(iv) the predominant role of the α-particle emission channel in the DNS disintegration; and

(v) the deformation of the heavy fragment at the scission point.

2. EXPERIMENTAL TECHNIQUE

The experiments were carried out at an external beam of the U-300 cyclotron of the JINR Laboratory of Nuclear Reactions. The ^{40}Ar ion energy was equal to 300 MeV, the average ion flux incident on the target was equal to 10^{12} particles per sec. The target was prepared from a natural silver foil 4.1 mg/cm^2 thick and placed in the entrance focus of a magnetic analyzer. The ^{40}Ar ion energy in the middle layer of the target was equal to 285 MeV. We recorded light transfer reaction products emitted at an angle of 40° in the angle interval of $\pm 2°$ and in the solid angle of 3×10^{-3} ster. The grazing angle was equal to 27°. The Z and A of the products were identified using magnetic analysis in combination with the ΔE-E technique [8]. The ΔE-E telescope was installed in the focal plane of the magnetic analyzer. A grid ionization chamber [9] was used as the ΔE detector. The product flight-path in the ionization chamber was equal to 100 mm, and the operating pressure was 100 torr. A gas mixture of 95% argon and 5% methane was used. The energy resolution of the ionization chamber for the elastically scattered ^{40}Ar ions (a gold target 0.3 mg/cm^2 thick) was about 3%. The surface-barrier full-absorption silicon detector E was placed into the ionization chamber and was not separated from the gas volume.

The pulses issued by the ΔE and E detectors were amplified and encoded to be fed to a MINSK-32 computer operated in the on-line mode. Coincidence in the ΔE and E detectors pulses were recorded on magnetic tape in 24-bit code. After each cycle of measurement, determined by the set of a certain number of pulses on the monitor, the results were fed to a digital printer in the form of two-dimensional spectra 128 (ΔE) to 64 (E) channels. The bombardment intensity was monitored by elastically scattered ions using a semiconductor detector placed at an angle of 30°.

The energy spectra of the isotopes were found by measuring the yield of reaction products at different values of the magnetic field of the spectrometer. The magnetic field was measured using the nuclear magnetic resonance method. The yields of isotopes in different charge states were summarized. The absolute values of the different cross sections $(d\sigma/d\Omega)_{40°}$ were found by normalizing the relative product yield to the cross section of the ^{40}Ar ions scattered elastically at small angles. A comparison of the obtained data with those of ref. [10], in which the same reaction was studied at 288 MeV, has shown a satisfactory agreement.

The visual examination of the targets after the bombardments showed the absence of carbonic films. Nevertheless we carried out a special bombardment of a carbon target 1 mg/cm^2 thick to detect different isotopes. This bombardment allowed one to conclude that the contribution to the products yield from the carbon film on the target was negligibly small.

3. EXPERIMENTAL RESULTS

3.1. Energy spectra

The energy spectra $(d^2\sigma/dE \cdot d\Omega)_{40°}$ of the isotopes of elements from Cl to He are shown in figs. 1, 2 and 3. The abscissa shows the total kinetic energy (TKE) of the conjugate pairs of fragments in the c.m. system. In converting the data from the laboratory system it was assumed that the products detected were produced by two-body reactions: 1 + 2 → 3 + 4. In the TKE calculations the ^{40}Ar ion energy (E_{lab} = 285 MeV) and the kinetic energy of the products were referred to the middle of the target. The mass number of the target was assumed to be equal to 108 (the silver is composed of 51.4% ^{107}Ag and 48.6% ^{109}Ag). Errors in the positions of experimental points represent the counting statistics. The arrow show the exit Coulomb barrier, B_c, calculated for spherical nuclei with an interaction radius R_{34} defined by the following relation:

$$R_{34} = 1.225 \times 10^{-13} \text{cm} \, (A_3^{1/3} + A_4^{1/3}) + 2 \times 10^{-13} \text{cm}. \qquad (1)$$

The thickness of the arrow characterizes the B_c variation with variation of mass number A_3 of the detected isotope of a given element Z_3.

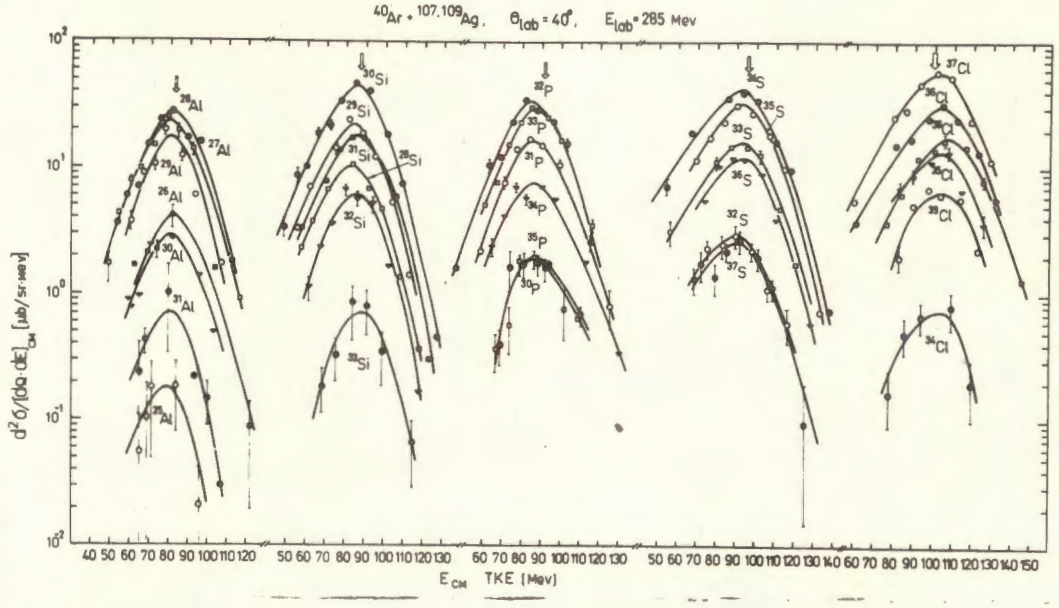

Fig. 1. Energy spectra of the $13 \leq Z \leq 17$ isotopes in the c.m. system, measured at a lab. emission angle of 40^{o} in the reaction Ag+ ^{40}Ar (E_{lab} =285 MeV). TKE is the total kinetic energy of the conjugate fragments. The arrows show the exit Coulomb barriers. The width of the arrow reflects the change in the Coulomb barrier with isotopic mass variations.

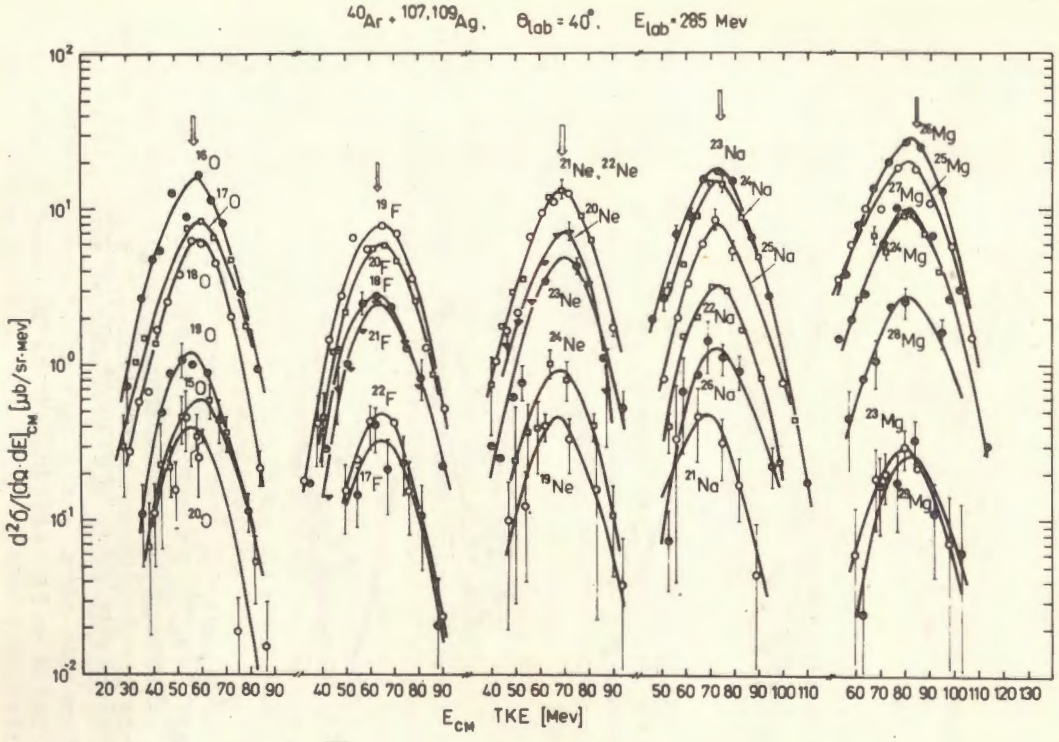

Fig. 2. Same as in fig. 1, for the isotopes of $8 \leq Z \leq 12$.

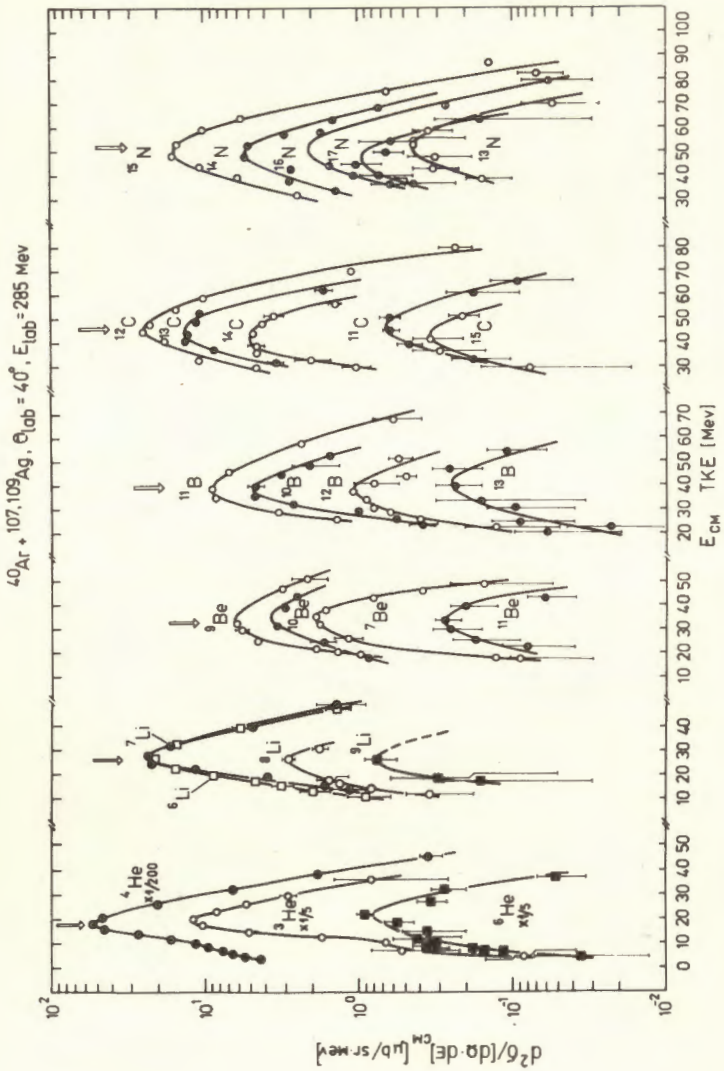

Fig. 3. Same as in fig. 1, for the isotopes of $2 \leq Z \leq 7$.

One can see in figs. 1-3 that the energy spectra of all the isotopes have the form of nearly symmetric curves with a maximum in the vicinity of the exit Coulomb barrier. This shape is characteristic of DIT reactions.

3.2. Differential cross sections for isotopic production

The Q_{gg} -systematics

Differential cross sections for the production of isotopes, $(d\sigma/d\Omega)_{40°}$ were obtained by integrating the energy spectra $(d\sigma/dE \cdot d\Omega)_{40°}$ over energy. The data obtained are presented in the Table.

The application of a statistical hypothesis to the DNS disintegration results in the following expression for isotopic production cross sections /1/

$$d\sigma/d\Omega \sim \exp \frac{Q_{gg} + \Delta E_c + \Delta E_{rot} - \delta(p) - \delta(n)}{T}, \qquad (2)$$

where $Q_{gg} = (M_1 + M_2) - (M_3 + M_4)$ is the energy consumed to reconstruct the nuclei, assuming that the final nuclei appear to be in their ground states; ΔE_c is a change in the DNS Coulomb energy, due to the redistribution of protons between the nuclei; ΔE_{rot} is a change in the DNS rotational energy owing to nucleon transfer, due to a variation of the DNS moment of inertia; $\delta(p)$ and $\delta(n)$ are the so-called non-pairing corrections, which help take account of the fact that the nucleons transferred from the donor nucleus pass to the excited levels of the acceptor nucleus; T is a parameter equivalent to the DNS temperature. If the quantity $Q_{gg} - \delta(p) - \delta(n)$ is plotted along the abscissa, and $\lg(d\sigma/d\Omega)$ is plotted along the ordinate, the cross sections for the production of the isotopes of a given element will lie on straight lines whose slope characterizes the DNS temperature. Fig.4 shows the Q_{gg} -systematics of cross sections for the production of isotopes of elements ranging from He to Ne. The two-isotopic composition of the silver target is taken into account by Q_{gg}. The production cross sections for isotopes of elements from Na to Cl are given in the same representation in fig.5. In fig. 6 the cross section $(d\sigma/d\Omega)_{40°}$ is given as a function of the neutron number N and proton number Z of the isotope. The data for ^{8}Be are obtained by extrapolation according to the Q_{gg} -systematics. Our attention has been drawn by the fact that the reaction chan-

Table

Detected isotopes, production cross sections ($d\sigma/d\Omega$) and Q values in the maximum of the energetic spectrum

-21	-20	-19	-18	-17	-16	-15	-14	-13	-12	-11	-10	-9	-8	NUMBER OF TRANSFERRED NEUTRONS
-8								19Ne 0014 141	20Ne 0242 139	21Ne 0528 139	22Ne 0548 135	23Ne 0183 137	24Ne 0035 140	
-9			A CHEL $(d\sigma/d\omega)_{lab}$(mb/sr) $-Q_{max}$				17F 0011 146	18F 0110 145	19F 0322 144	20F 0224 143	21F 0080 144	22F 0016 144		
-10						15O 0021 147	16O 0584 149	17O 0327 147	18O 0234 148	19O 0042 152	20O 0018 152			
-11					13N 0021 153	14N 0235 153	15N 0638 153	16N 0087 151	17N 0029 158				34Cl 0039 116	35Cl 0720 108	36Cl 1801 104	37Cl 2088 109	38Cl 1000 104	39Cl 0354 110	40Cl 0041
-12				11C 0023 156	12C 0938 159	13C 0486 157	14C 0178 160	15C 0012 164				32S 0168 118	33S 1074 117	34S 2298 114	35S 1749 116	36S 0615 118	37S 0131 120		-2
-13				10B 0143 167	11B 0307 169	12B 0038 169	13B 0007 165				30P 0079 120	31P 0922 120	32P 1728 123	33P 1444 120	34P 0390 123	35P 0098 120			-3
-14		7Be 0049 173		9Be 0310 175	10Be 0143 174	11Be 0009 173			27Si 0004	28Si 0488 123	29Si 0736 124	30Si 2145 121	31Si 0915 120	32Si 0276 124	33Si 0072 125				-4
-15		6Li 0456 181	7Li 0475 181	8Li 0096 181	9Li 0010 182			25Al 0007 133	26Al 0190 132	27Al 1082 127	28Al 1211 128	29Al 0615 129	30Al 0133 127	31Al 0032 129					-5
	3He 1006 188	4He 2230 189	6He 1087 187				23Mg 0009 129	24Mg 0363 128	25Mg 0856 128	26Mg 1156 127	27Mg 0426 127	28Mg 0105 128	29Mg 0012 128						-6
						21Na 0010 140	22Na 0122 135	23Na 0725 135	24Na 0576 134	25Na 0328 135	26Na 0051 136	27Na 0011							-7
NUMBER OF TRANSFERRED NEUTRONS						-12	-11	-10	-9	-8	-7	-6	-5	-4	-3	-2	-1	0	+1

NUMBER OF TRANSFERRED PROTONS

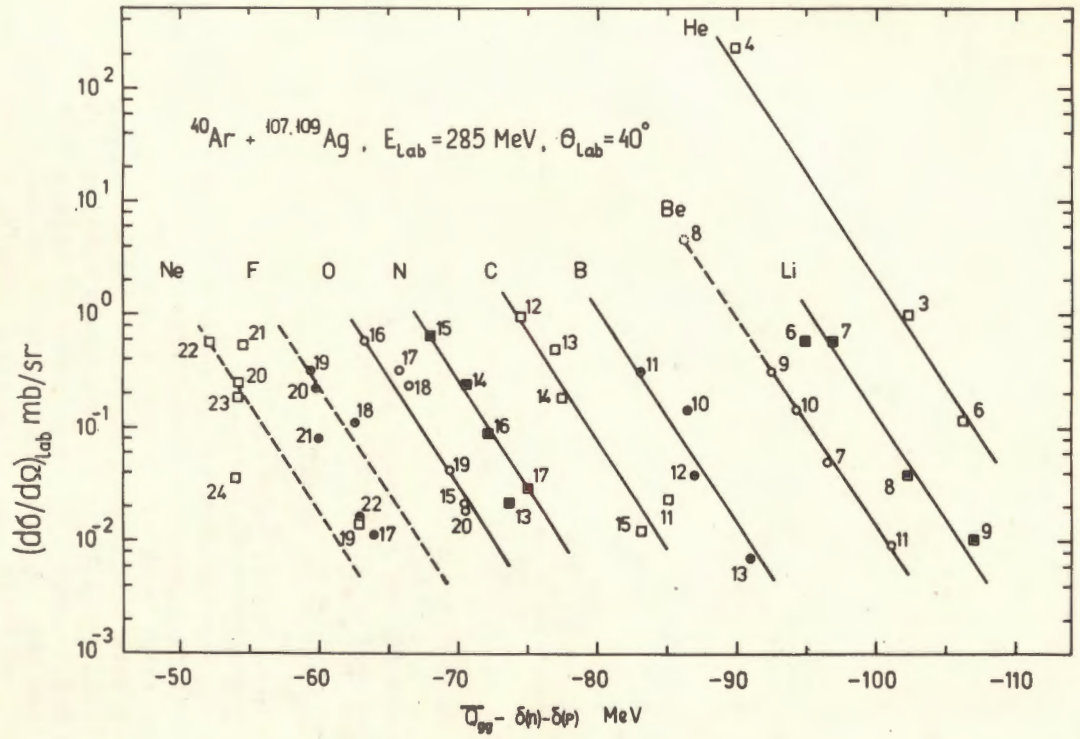

Fig. 4. The Q_{gg}-systematics of the differential cross sections for the production of isotopes of $2 \leq Z \leq 10$ in the reaction $^{107,109}Ag + ^{40}Ar$(285 MeV), $\theta_{lab} = 40^{\circ}$.

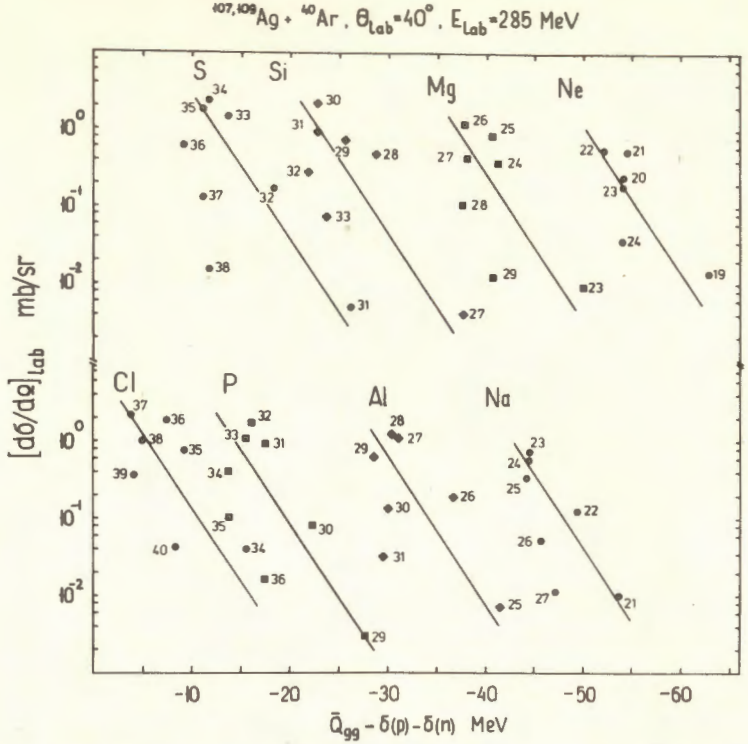

Fig. 5. Same as in fig. 4, for isotopes of $11 \leq Z \leq 17$.

nel involving the α-particle emission strongly dominates over the rest of the multinucleon transfer channels.

4. DISCUSSION OF RESULTS

4.1. The Q_{gg}-systematics

The Q_{gg}-systematics of the cross sections for the production of isotopes in transfer reactions induced by heavy ions has first been established in ref. /11/ . The Q_{gg}-systematics were interpreted using the concept of partial statistical equilibrium /12/ which was naturally justified by the DNS concept /13/ . In a number of papers /14-19/ it was shown that the Q_{gg}-systematics hold for target nuclei from ^{12}C to ^{232}Th and projectiles from ^{11}B to ^{22}Ne. However, the first experiment with the heavier ions has failed /20/ . At Orsay, ^{232}Th was bombarded with the

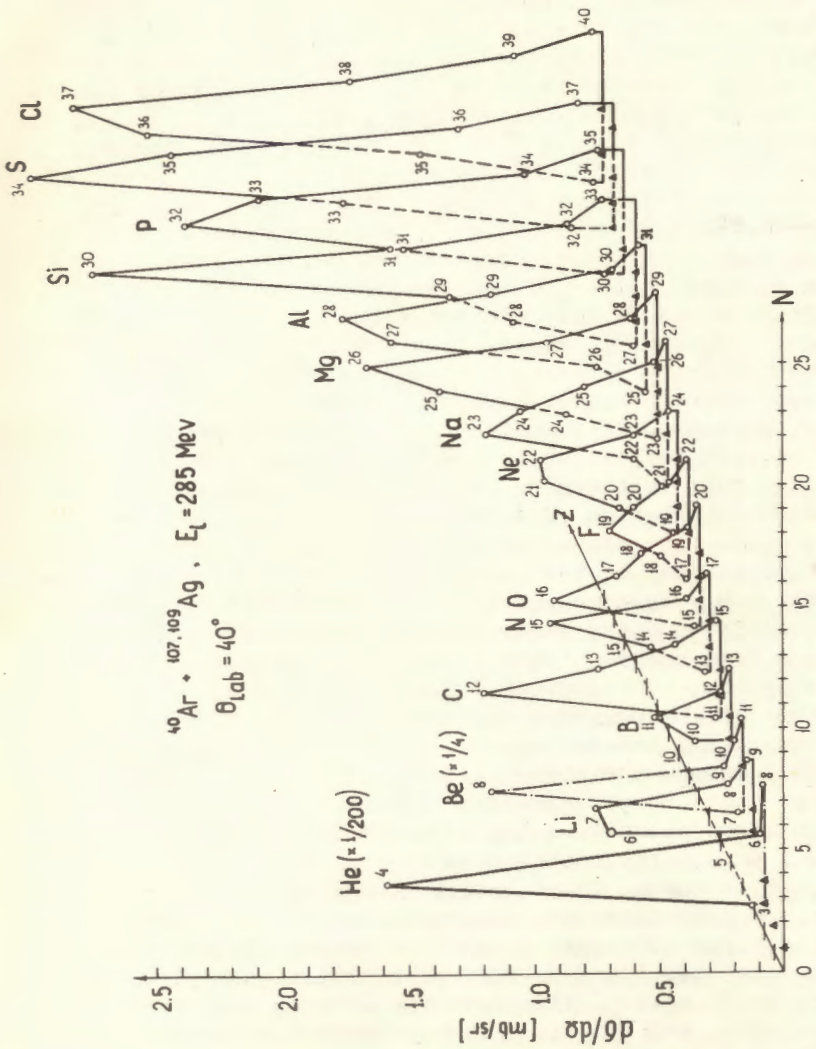

Fig. 6. Differential cross sections for the production of isotopes of $2 \leq Z \leq 17$ as a function of the neutron number **N** and proton number Z of the isotope, in the reaction ^{107,109}Ag+^{40}Ar (285 MeV), θ_{lab}=40°. Stable isotopes are indicated with closed triangles.

295 MeV ^{40}Ar ions. The cross sections for the production of isotopes of elements from Mg to Ti have been measured, which did not obey the characteristic exponential dependence of $d\sigma/d\Omega$ on the quantity Q_{gg}. At the same time, the applicability of the Q_{gg}-systematics for the description of the isotopic production cross sections in transfer reactions with the heaviest ions is of special interest. For very heavy ions, the contribution of DIT reactions to the reaction cross sections σ_R increases, and these reactions become a predominant nuclear process /6/.

Our experiments using ^{40}Ar ions differed from those carried out in ref./20/ in two respects. First, we detected the isotopes of lighter elements. This allowed us to reduce the effect of sequential nuclear processes such as nucleon and α-particle evaporation. Second, the range of the measured values of cross sections was one order of magnitude wider. From the data obtained (Fig. 4) one can see that the Q_{gg}-systematics are satisfied for the isotopes of light elements inclusive of oxygen, whereas the Q_{gg}-systematics are violated for the isotopes of the heavier elements. It should be noted that the production cross section for helium isotopes also obeys the Q_{gg}-systematics. This fact can be regarded to be indicative of the main contribution of multinucleon transfer reactions to the production of helium isotopes. The regular character of deviations of the isotopic production cross sections from the Q_{gg}-systematics (fig.5) indicates the effects of sequential nuclear processes and, mainly, neutron evaporation from excited light fragments. Neutron evaporation from a neutron-rich isotope is responsible for the displacement of the corresponding point on the Q_{gg}-systematics toward the smaller values of $|Q_{gg}|$. In neutron-deficient isotopes the strong binding energy of neutrons prevents their evaporation from the nucleus. However, neutron evaporation from the adjacent isotopes of N larger by 1 or 2 units contributes to the yield of neutron-deficient isotopes. This contribution displaces the points of the Q_{gg}-systematics, corresponding to neutron-deficient isotopes, upwards, toward the larger values of $d\sigma/d\Omega$. For the isotopes lying in the valley of β-stability, Q_{gg} depends on N weakly. Therefore the neutron evaporation process will lead only to a redistribution of the yields of the isotopes without changing noticeably their positions with respect to the abscissa axis.

The experimental data obtained in the present paper allow one to conclude that in the reactions induced by ^{40}Ar ions the Q_{gg}-systematics are fulfilled for the cross sections of the DIT primary products. Our calculation /21/ taking neutron evaporation into account, based on the experimental data described in ref. /22/, has shown that in the case of Kr and Xe ions the Q_{gg}-systematics also describe the relative yield of multinucleon transfer reaction products. Thus, the Q_{gg}-systematics represent one of the most general regularities of the DNS disintegration and reflect the statistical aspect of the DIT mechanism.

4.2. The excitation energy of the light fragment

We have tried to use the deviation of the isotopic production cross section from the Q_{gg}-systematics to estimate the thermal excitation energy of the light fragment and, consequently, of the distribution of thermal energy between the DNS fragments.

In such calculations it was assumed that the primary distribution of the isotopic production cross sections obeyed the Q_{gg}-systematics. Then the probability of evaporation of one to four neutrons, a proton, and α-particle as a function of the excitation energy of the isotope was calculated using a Monte-Carlo method in the fermi-gas approximation /23,24/. The results of the calculation are presented in fig. 7. The isotope excitation energy was chosen to be such that the primary distribution of isotopic cross sections be transformed to the experimentally observed one. The slope of the lines of the elements treated in the calculation was taken to be the same as that of the light elements that obeyed the Q_{gg}-systematics. To determine the position of the primary line of an element on a plane with axes $\lg(d\sigma/d\Omega)$ and $Q_{gg} - \delta(p) - \delta(n)$ we assumed the equality of the sums of the production cross section of isotopes of a given element, calculated according to the Q_{gg}-systematics and those measured experimentally. The calculations have shown that neutrons played a predominant role in removing the excitation energy. As to the probability of the emission of different particles from excited light fragments, our data are in satisfactory agreement with the results of ref. /25/ in which DIT reactions were studied in the system Ag + ^{40}Ar (340 MeV) by the correlation method.

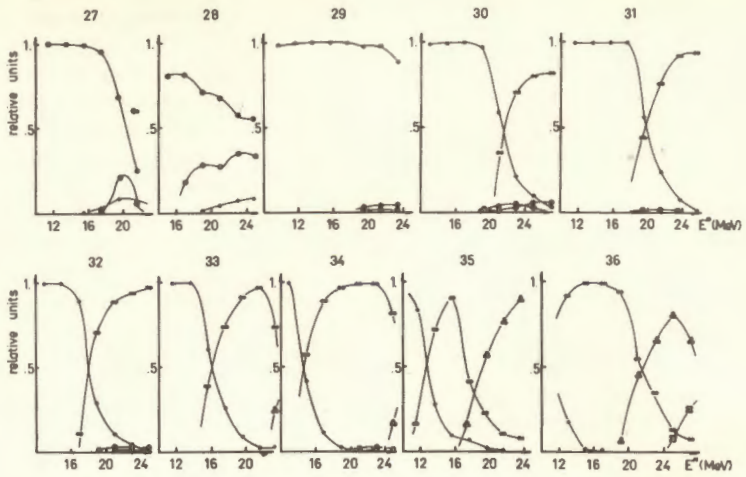

Fig. 7. Probability of evaporation of one (·), two (··), three (⋱) and four (⁘) neutron, a proton (•) and α-particle (o) from the excited Si isotopes as a function of excitation energy.

The results of the calculation of thermal excitation energy for isotopes of elements from F to Cl are presented in fig. 8. The value of the thermal energy of the light fragment, calculated assuming its proportionality to the fragment mass is also shown in fig. 8. In calculating the thermal excitation energy of the DNS the rotational energy of the system and the Q_{gg} value were taken into account.

From fig. 8 it is seen that there is a substantial difference in the estimates of the excitation energy of the light fragment by two different methods. In our view, this difference can be explained in the following way. In the DNS, the carriers of thermal excitation energy are the excited nucleons belonging to the exchange zone /1/. These nucleons can easily pass from one nucleus to the other, and their wave function is common for both nuclei. In the stripping reactions detected by us, the nucleons of the light fragment gradually pass to the target nucleus, in which they leave part of their kinetic energy, and settle on the lower excited levels. Together with nucleons, the light nucleus looses part of its thermal energy and becomes cooled. This may be an explanation of the decrease in the thermal excitation energy of the light fragment

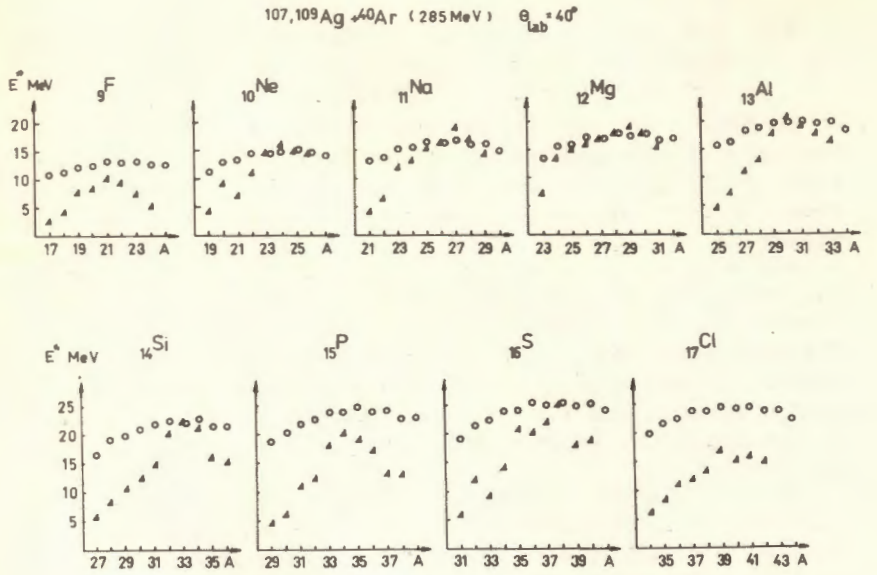

Fig. 8. The results of calculation for the thermal excitation energy of light fragments from the DNS disintegration in the reaction $^{107,109}Ag + ^{40}Ar$ (285 MeV), $\theta_{lab} = 40^{o}$. The closed triangles indicate the data obtained from the deviations of the isotopic production cross sections from the Q_{gg} -systematics. The open circles are the data obtained from the distribution of thermal energy proportionally to the fragment mass.

in the case of neutron transfer to the target nucleus. The decrease of excitation energy in very neutron-rich isotopes seems to have another reason. The production of these isotopes is connected with the transfer of neutrons from the target nucleus to the projectile, or with the keeping of most of the neutrons in the projectile. It is known /4/ that the large angular momentum of the DNS favours such a direction of neutron transfer. One can think that the main contribution to the production of these isotopes comes from collisions with the higher angular momenta. An increase in the angular momentum of the DNS leads to an increase in the rotational energy and a decrease in the thermal energy of the system. Correspondingly the thermal energy of the light fragment also decreases.

4.3. The nuclear structure effects on the yield of DIT products. The predominant role of the reaction channel involving ^4He emission

In fig. 6 one can notice the following characteristic features of the dependence of the differential cross section $(d\sigma/d\Omega)_{40^\circ}$ on Z and N of the isotope. Initially the cross section for the production of isotopes with maximum yields up to fluorine decreases as Z decreases. Such a tendency corresponds to the predictions of the theoretical models in which nucleon exchange between the nuclei is considered as a diffusion process /4,5/ . The farther Z of the fragments from Z of the initial nucleus, the longer time is required for the DNS to achieve the corresponding configuration, and the smaller cross section is expected. In the first diffusion models the shell structure of nuclei was neglected.

On the contrary, following fluorine the cross sections increase as Z decreases. This increase is especially pronounced for nuclei with closed shells and subshells, such as ^{16}O, ^{15}N, ^{12}C, ^4He as well as for ^8Be. The cross section reaches its maximum value, 220 mb, for ^4He. The production cross section for ^4He is two orders of magnitude as large as the cross section for the production of any of the isotopes detected. The isotopic yield also shows the Z and N partly effects. The even-Z isotopes show larger cross sections as compared with the adjacent odd-Z isotopes. All the even-Z isotopes have maximum yields for the even values of N. For most of odd-Z isotopes the maximum also corresponds to an even value of N.

The unusually sharp increase of the ^4He production cross section was also observed in our previous works /14,15/, where a large number of isotopes including the heavy helium isotopes ^6He and ^8He were detected as multinucleon transfer reaction products. By using the yield of these isotopes and the Q_{gg} -systematics one could make reliable estimates for the ^4He yield due to multinucleon transfer reactions. We thought it appropriate to present these data here, fig. 9.

One can indicate two factors associated with nuclear structure, which influence the yield of multinucleon transfer reactions. These are the magnitude of the DNS potential energy and an enhanced stability of nuclei with closed shells. In Fig. 10, the DNS potential energy is shown as a function of the Z and A of the light fragment.

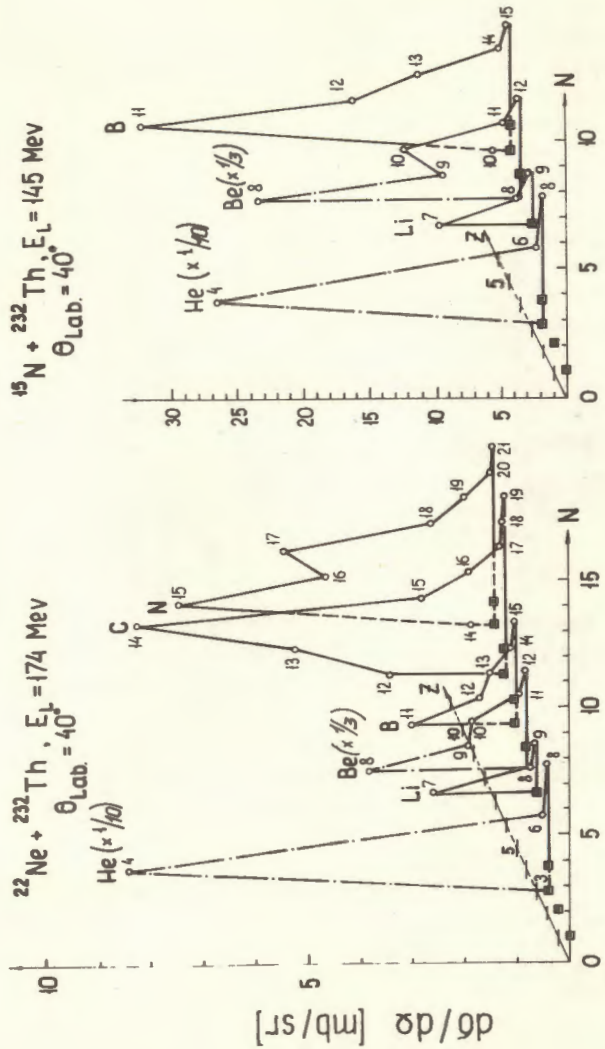

Fig. 9. Differential cross sections $(d\sigma/d\Omega)_{40^\circ}$ for the production of isotopes of $2 \leq Z \leq 7$ in the reaction $^{232}Th + ^{22}Ne$ (174 MeV) /15/ and of isotopes of $2 \leq Z \leq 5$ in the reaction $^{232}Th + ^{15}N$ (145 MeV) /14/. In both reactions $\theta_{lab} = 40^\circ$.

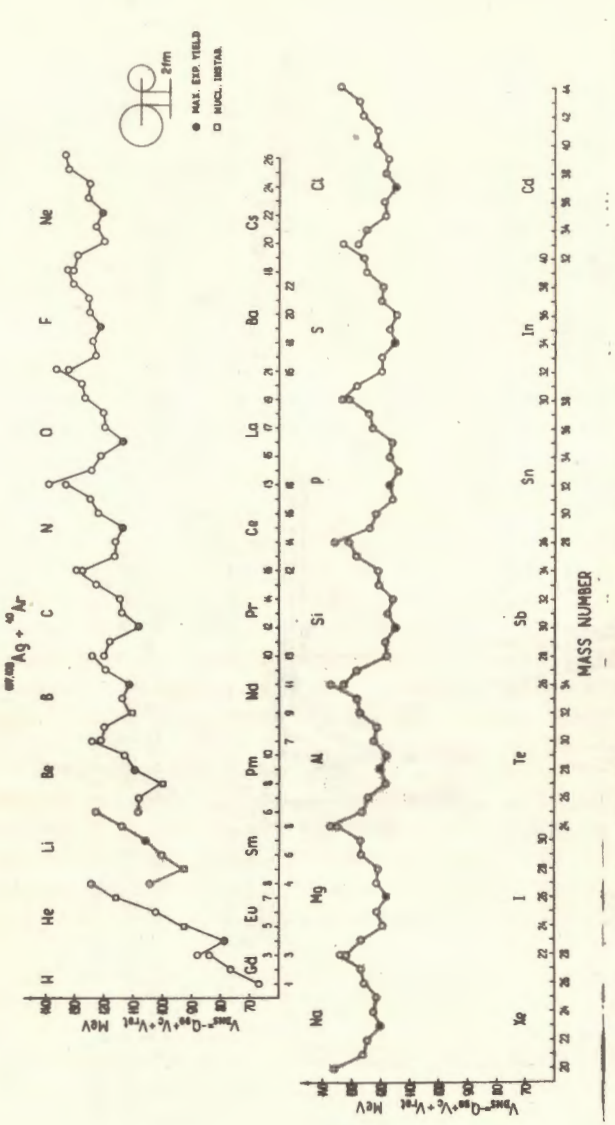

Fig. 10. The DNS potential energy as a function of A and Z of the light fragment. The chemical symbol of the conjugated heavy fragment is also indicated. The calculation is done for spherical fragments with the distance of closest approach of 2 fm and for initial angular momentum ℓ_i =110. The nuclear masses are taken from ref. /26/ . Only an excess of the fragment mass over that of the initial nuclei is taken into account. "Sticking" limit was used.

In the calculation the shape of the DNS was approximated by two spheres. The nuclear masses were taken from the tables of ref. /26/ . The angular momentum of collision was taken to be equal to 110h. "Sticking" limit was used.

From fig. 10 one can see that each Z value of the light fragment corresponds to the mass number A for which the DNS potential energy has a minimum value. This minimum in turn corresponds to the maximum cross section for the isotopes of a given element. The deepest minimum stands for the α -cluster configuration of the DNS. Therefore, in the course of its evolution the DNS will tend to assume this configuration.

Another aspect of the shell structure on the DNS evolution is illustrated in fig. 11. In ^{40}Ar nucleons fill the 1s, 1p, 2s, 1d, and 1f shells. It may be expected that at the moment of nuclear collision the nucleons of the upper shells get excited in the first place. The binding energy of the nucleons of these shells is lower, and their wave functions are concentrated closer to the nuclear surface.

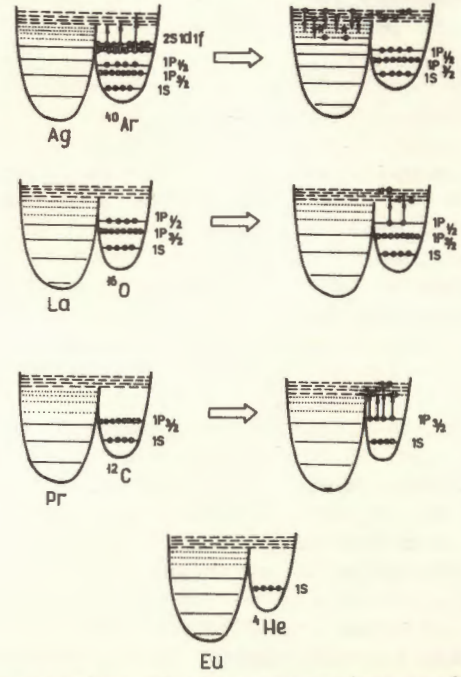

Fig. 11. Illustration of the successive excitation and transfer of nucleons from different shells of the ^{40}Ar nucleus.

The excited nucleons pass to the exchange zone, where they can easily travel from one nucleus to the other. In the stripping reactions, the excited nucleons are gradually concentrated in the target nucleus, settling on the lower excited levels. This denudes the p-shell of the light nucleus, and, as a result, a configuration consisting of the unexcited ^{16}O nucleus and the conjugate excited lanthanum nucleus is formed. In order that the DNS might evolve further, it is necessary to break the pair and transfer the proton from the $p_{1/2}$ subshell to the exchange zone. The coupling energy in the ^{16}O nucleus exceeds 6 MeV, and apparently some time is required for this nucleus to obtain sufficient excitation. The evolution of the DNS will be delayed, and this in turn will lead to an enhanced yield of the ^{16}O nuclei. A similar situation occurs when the light fragments appear to be the ^{12}C, ^{8}Be and ^{4}He nuclei. The masses of these nuclei are smaller than that of ^{16}O. Correspondingly, their fraction of thermal energy is also smaller than in the case of ^{16}O. On the contrary, the energy required to break the pair increases to 9.6, 16.6 and 19.8 MeV, respectively.

4.4. Dynamical deformation of the double nuclear system

It is generally accepted that DIT reactions occur in collisions at angular momenta in the range of ℓ_{cr}, $\ell_{cr}+\Delta\ell$. For the system Ag + ^{40}Ar, the critical angular momentum ℓ_{cr} was measured experimentally in ref.[27]. It was equal to 108 ± 8 at an energy of 228 MeV. However, in ref.[27] the contribution of "direct" α-particles to the incomplete fusion cross section was not taken into account. In our measurements the production cross section for "direct" α-particles is equal to 300 mb, which leads to a decrease of ℓ_{cr} to 96. The $\Delta\ell$ value was estimated from the total cross section of all DIT channels including the cross section for the production of "direct" α-particles, $\Delta\ell$ =30. Thus, the average angular momentum in the entrance channel in DIT was equal to ℓ_i =111. The DNS with such a large angular momentum should experience a considerable dynamical deformation, which can be estimated from the energy spectra (fig. 1-3).

Under the "sticking" conditions, which occur in our case, the total kinetic energy of the fragments is determined by the sum of the exit Coulomb and centrifugal barriers for a deformed DNS, i.e.,

$$TKE = B_c^{def} + B_{rot}^{def} . \quad (3)$$

The excitation energy of the DNS in the reaction investigated is about 80 MeV. Therefore the moment of inertia of the system can be assumed to be a rigid-body one. The initial angular momentum is distributed between the spins of the fragments and the orbital angular momentum proportionally to the corresponding moments of inertia.

The rapidity rotating DNS takes on a rather complicated shape. For the sake of simplicity of calculations, the shape of the light fragment was assumed to be spherical, while that of the heavy one to be a prolate rotational ellipsoid. This assumption is rather realistic since most of the initial angular momentum is converted to the spin of the heavy fragments, which reaches many tens of $\hbar$.

The deformation calculations were performed for the isotopes with maximum yields and for TKE in the maxima of the energy spectra. The results of the calculation for the deformation of the heavy fragment at the moment of the DNS disintegration are shown in fig. 12. The atomic numbers of the light fragment, Z_3, and of the heavy fragment, Z_4, are plotted along the abscissa; the spins of the fragments I_3, I_4 are indicated. The large-to-small semiaxis ratio is plotted along the ordinate. For the purpose of comparison with other works in which deformation is expressed in terms of parameter r_0 for the radius of the interaction of the spherical final nuclei, the data on this parameter are also presented. As one can see from the data obtained, the dynamical deformation of heavy fragments in DIT reactions may reach rather large values. The large-to-small semiaxis ratio approaches three. The deformation increases with the number of the nucleons transferred to the target nucleus, which seems to be associated with an increase in the spin of the heavy fragment.

Quite recently it has been believed that a large deformation at the scission point is a "privilege" of the heaviest ions such as Kr and Xe. This formed a basis for introducing the term "quasifission" for the new type of reactions between complex nuclei. The analysis of the DNS deformation taking into account the rotational energy of the system has shown that in this respect there is no difference between quasifission and DIT reactions either.

To conclude this section we would like to draw one's attention to the fact the DIT reactions may be used to study the dynamical deformation of fast rotating nuclei.

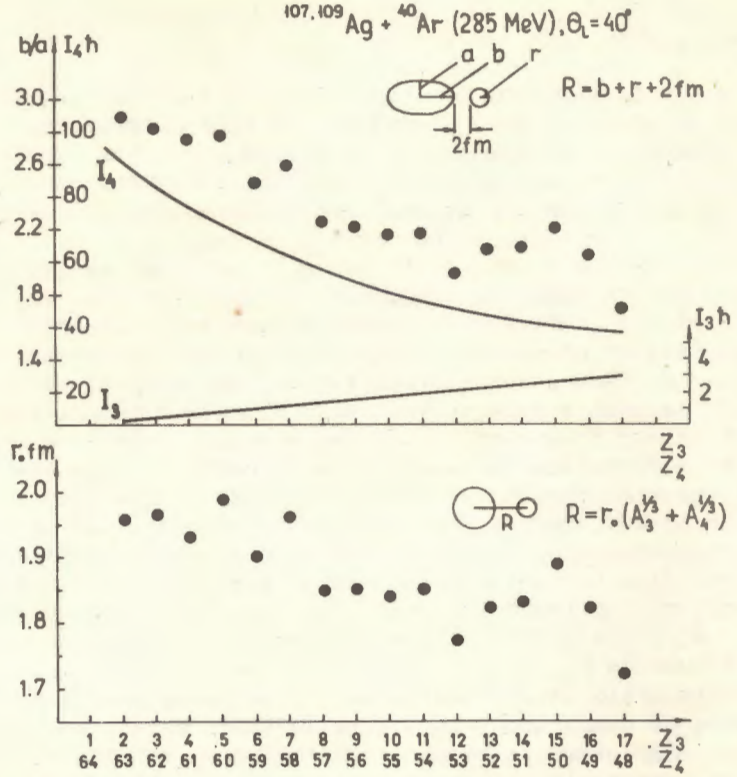

Fig. 12. Estimated dynamical deformation of heavy fragments during the DNS disintegration in the reaction $^{107,109}Ag + ^{40}Ar$ (285 MeV), $\theta_{lab} = 40^{o}$. Z_3 and Z_4 are the atomic numbers of the light and heavy fragments, respectively, and I_3 and I_4 are their spins. The corresponding values of the effective parameter r_0 are shown in the lower part.

If one records a rigid nucleus, say ^{16}O or ^{4}He, as a light fragment, it is possible to estimate the deformation on the heavier conjugate nucleus from the value of TKE.

5. CONCLUSION

Deep inelastic transfers have been studied in the system $^{107,109}Ag + ^{40}Ar$ (285 MeV). The energy spectra and differential cross sections of 87 isotopes of elements ranging from He to Cl were measured at an emission angle of 40^{o}.

It has been established that the Q_{gg}-systematics are satisfied in deep inelastic transfer reactions induced by ^{40}Ar ions. Their violation is connected with the effect of sequential nuclear processes such as the evaporation of nucleons and α-particles from the excited fragments.

It has been revealed that the dependence of the excitation energy of the light fragment on its mass number is different from that based on the distribution of thermal energy between fragments proportional to their masses. It has been established that the nuclear structure of the light fragment influences the magnitude of its production cross section, under the conditions of the high excitation energy of the DNS. It has been established that the reaction channel involving the emission of α-particles strongly dominates over the other channels of multinucleon transfer reactions. This is indicative of the important role of the α-cluster configuration in the evolution and disintegration of the DNS. The data obtained permit a new insight into the process of the DNS evolution and the fusion of two complex nuclei, and reveal one of the most important mechanisms of the formation of "direct" α-particles in heavy ion reactions.

It is shown that in DIT reactions the heavy fragment may experience a considerable dynamical deformation. In the rotational ellipsoid representation the ratio of the large axis to the small axis can amount to three. A possibility of using DIT reactions for investigating the deformation of fast rotating nuclei is under discussion.

ACKNOWLEDGMENTS

The authors are pleased to thank Academician G.N.Flerov for his stimulating interest and critical comments on the paper, the cyclotron staff for an efficient operation of the U-300 cyclotron during the experiments, E.A.Cherepanov for discussions and for providing programmes for the calculation of nucleon evaporation from excited nuclei, and L.Pashkevich for preparing an English version of the text.

REFERENCES

1. Volkov V.V. Physica Reports, 1978, 44, p.93.
2. Schröder W.V., Huizenga J.R. Ann.Rev.Nucl.Sci., 1977, 27, p.465.
3. Galin J. J. de Phys., 1976, 37, C5-83.

4. Moretto L.G., Schmitt R. J. de Phys. ,1976, 37, C5-109.
5. Nörenberg W. J de Phys., 1976, 37, C5-141.
6. Bock R. Proc. Intern. Conf. on Nuclear Structure. Tokyo, September 5-10, 1977. Supp. to the J. Phys. Soc. ,Japan, 1978, 44, p.730.
7. Lefort M., Ngo Ch., Ann.Phys., 1978, 3, p.5.
8. Artukh A.G. et al.Nucl.Instr. and Meth., 1970, 83,p.72.
9. Artukh A.G. et al. Yad. Fiz., 1978, 27, p.29.
10. Galin J. et al. Nucl.Phys., 1975, A255, p.472.
11. Artukh A.G. et al. Nucl.Phys., 1971, A160, p.511.
12. Bondorf J.P. et al. J de Phys., 1971, 32, C6-145.
13. Volkov V.V. Proc. Intern. Conf. on Reactions Between Complex Nuclei, Nashville, 1974, vol. 2 eds. R.L.Robinson et al. (North-Holland, New York, 1874) p.363.
14. Artukh A.G. et al. Phys. Lett., 1970, 33B, p.407.
15. Artukh A.G. et al. Nucl.Phys., 1973, A211, p.299.
16. Volkov V.V. Nucleonica, 1976, 21, p.53.
17. Mikheev V.L. et al. Yad.Fiz., 1977, 25, p.255.
18. Mikumo T. et al. Proc. INS-IPCR Symposium on Cluster Structure of Nuclei and Transfer Reactions Induced by Heavy Ions. Tokyo 1975, ICPR Cyclotron Progress Report, supplement 4, p.617.
19. Cormier T.M. Proc. of the Symposium on Macroscopic Features of Heavy-Ion Collisions 1-3 April 1976, vol.1, p. 153, ANL/PHY-76-2.
20. Jacmart J.C. et al. Nucl.Phys., 1975, A242,p.175.
21. Cherepanov E.A. et al. JINR, E7-11364, Dubna 1978.
22. Oganessian Yu.Ts. et al. Yad.Fiz., 1973, 18, p.734.
23. Iljinov A.S. et al. Z.Phys., 1978, A287, p.37.
24. Barashenkov V.S. et al. JINR, P7-6741, Dubna 1972.
25. Cauvin B. et al. Nucl.Phys., 1978, A301, p.511.
26. Kravtsov V.A. Atomic Masses and Nuclear Binding Energies, (Atomizdat, Moscow, 1974).
27. Britt H.C. et al. Phys.Rev., 1976, C13, p.1483.

Received by Publishing Department
on April 21 1979.